# Embedded optical waveguides fabricated in SF10 glass by low-repetition-rate ultrafast laser

Jing Bai,[1,2] Xuewen Long,[1,2] Xin Liu,[1] Guangwen Huo,[1] Wei Zhao,[1] Razvan Stoian,[3] Rongqing Hui,[4] and Guanghua Cheng[1,*]

[1]State Key Laboratory of Transient Optics and Photonics, Xi'an Institute of Optics and Precision Mechanics, Chinese Academy of Sciences, Xi'an 710119, China

[2]Graduate University of Chinese Academy of Sciences, Beijing 100049, China

[3]Laboratoire Hubert Curien, UMR 5516 CNRS, Université de Lyon, Université Jean Monnet, Saint Etienne 42000, France

[4]Department of Electrical Engineering and Computer Science, University of Kansas, Lawrence, Kansas 66044, USA

*Corresponding author: gcheng@opt.ac.cn

Symmetric embedded waveguides were fabricated in heavy metal oxide SF10 glass using slit-shaped infrared femtosecond laser writing in the low-repetition frequency regime. The impact of the writing parameters on the waveguide formation in the transverse writing scheme was systemically studied. Results indicate that efficient waveguides can be inscribed in a wide parameter space ranging from 500 fs to 1.5 ps pulse duration, 0.7–4.2 μJ pulse energy, and 5 μm/s to 640 μm/s scan speed and pointing out the robustness of the photoinscription process. The refractive index profile reconstructed from the measured near field pattern goes up to $10^{-3}$. In addition, propagation losses of the waveguides are tolerable, with the lowest propagation loss estimated at 0.7 dB/cm. With a 5 μm/s scan speed and 3.5 μJ pulse energy in a high-dose regime, few-mode guiding was achieved in the waveguide at 800 nm signal injection wavelength. This is due to a combination of increased refractive index in the core of the trace and the appearance of a depressed cladding. © 2013 Optical Society of America

*OCIS codes:* (140.3390) Laser materials processing; (220.4000) Microstructure fabrication; (130.2755) Glass waveguides.

http://dx.doi.org/10.1364/AO.52.007288

## 1. Introduction

Since the demonstration of ultrafast laser refractive index modification inside bulk glasses [1], direct ultrafast laser writing (DLW) has proven to be a practical and powerful technique for three-dimensional (3D) volume microstructuring of transparent dielectric media [2]. In the index-modification process, non-linear absorption confines laser interactions to the focal volume, leading to permanent refractive index changes in the irradiated region or in the neighboring zones, depending on the rate of exposure. This allows optical waveguides to be fabricated with a certain control on the index profile. The performance of the waveguides fabricated by ultrafast laser inscription depends on the ultrafast laser pulse (wavelength, pulse energy, pulse duration, repetition rate, and polarization) and on processing conditions (scan speed, focal depth, and irradiation geometry), as well as on the material response (substrate material properties) [3]. This technique has been successfully applied to fabricating channel waveguide devices in a wide variety of transparent materials, including glasses, crystals, ceramics, and polymers [4–13].

SF10 glass, part of the broader heavy metal oxide (HMO) glasses family, has attracted much attention owing to its advantageous features, such as reduced

phonon energies for DLW, an extended transparency window from UV to the mid-infrared, high densities, low glass transition temperatures, and excellent chemical and physical stability. SF10 glass is also known for its low melting point (about 450°C), high nonlinear refractive index ($10^{-19}$ m$^2$/W), and two-photon absorption corresponding to relatively small energy band gaps (2–3 eV) and thus should allow for control over the refractive index change through the variation of laser writing conditions. Recently, Siegel *et al.* [14] demonstrated that efficient optical waveguides can be fabricated in $35PbO \cdot 35Bi_2O_3 \cdot 15Ga_2O_3 \cdot 15GeO_2$ glass by 1 kHz femtosecond (fs) laser through the stress-induced mechanisms, yielding a refractive index change surpassing $10^{-3}$. Furthermore, similar waveguide structures have also been created in HMO glass such as SF57 glass [15]. Because of the high thermo-mechanical expansion coefficient (about $100 \times 10^{-7}$) of HMO glass, both concepts rely on the stress/compaction-induced positive refractive index change, which always emerges in the vicinity of several damaged tracks. More recently, Thomson *et al.* [16] reported the formation of high-gain waveguide amplifiers in Er-doped bismuthate glass (>70% wt% $Bi_2O_3$) by the multiscan of a 500 kHz repetition rate fs laser. To our knowledge, there has not yet been any report on the formation of light guidance within a single track in HMO glasses, particularly SF10, by low-repetition-rate ultrashort pulse. We point out that embedded waveguides in SF10 glass, which also possess excellent transparency in the mid-infrared and high nonlinear refractive index, can show potentially promising features for the development of 3D integrated photonic devices operating in the mid-infrared and potential application in nonlinear optics phenomenon research.

In this paper, we report the fabrication of embedded optics waveguide in SF10 glass using a slit beam shaping method [17], indicating a soft photosensitivity regime. We demonstrate that a positive change in the refractive index is produced within the laser irradiation trace in SF10 glass by an ultrafast laser pulse without stress assistance. A wide range of laser exposure conditions was examined, revealing waveguide formation in a relatively large processing parameter space ranging from 500 fs to 1.5 ps in pulse width, 0.7–4.2 µJ in pulse energy, and 5 µm/s to 640 µm/s in scan speed, indicative of a robust photoinscription process. The waveguides are characterized by near-field mode profiles, and the lowest propagation loss is found to be 0.7 dB/cm at the 980 nm wavelength. Increasing the dose, with a scan speed of 5 µm/s, pulse energy of 3.5 µJ and pulse duration of 1.2 ps, the few-mode guiding was observed by 800 nm laser injection. This relative increase of the normalized frequency was due to the achievement of a large overall refractive index contrast via increasing the refractive index in the core and onsetting a decreased index in a surrounding depressed cladding.

## 2. Experimental Setup

The schematic description of the experimental setup is shown in Fig. 1. A regeneratively amplified Ti: Sapphire ultrafast laser system (Spitfire, Spectra Physics) was used to expose a bulk SF10 glass sample in the experiment. The central wavelength of the output laser pulses is 800 nm and the pulse repetition rate is 1 kHz. The pulse duration can be varied from 120 fs to 1.5 ps by tuning the compressor grating position while monitoring the positively chirped pulse duration with an autocorrelator (APE Pulse Check). A shutter is used to control the irradiation time of the laser pulses in the sample. The pulse energy is controlled with a half-wave plate placed before a polarizer. Polished samples of SF10 glass (Schott 65997-17-3, 20 mm × 10 mm × 4 mm) were employed, mounted on a computer-controlled XYZ motion stage (Physik Instrumente) that allows translation parallel or perpendicular to the laser-propagation axis. The laser beam was focused inside the target by a long-working-distance 20× Mitutoyo microscope objective (working distance 20 mm, nominal numerical aperture NA = 0.42, and 70% transmissivity at 800 nm). A transverse writing configuration, with translation perpendicular to the laser propagation axis, was used in the experiment throughout the text unless stated otherwise. A slit with 500 µm width was positioned before the focusing objective in order to produce highly symmetric waveguide cross-sections allowing also for a fine tune and the achievement of low exposure doses (focusing y, z waists of 0.5 and 5 µm, respectively). Note that the pulse energies on the target mentioned in the following text were measured values after passing through the slit and objective. An Olympus BX51 positive phase-contrast microscope (PCM) was employed to monitor the interaction region in a side-view geometry. In this arrangement, the relative positive index changes appear dark on a gray background while white zones indicate negative index variations or scattering centers. The real-time PCM monitoring
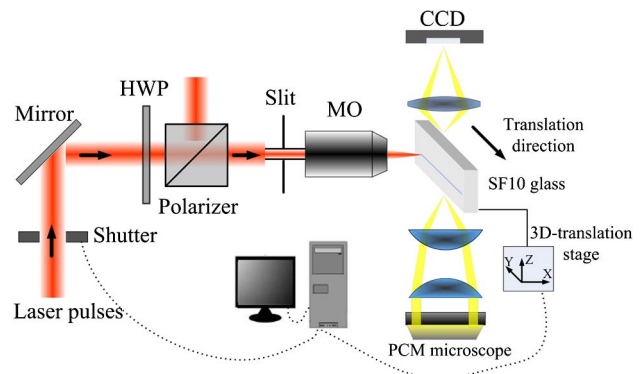


Fig. 1. Experimental setup of the femtosecond laser waveguide writing arrangement indicating the irradiation geometry and glass sample orientation: MO, microscope objective; HWP, half-wave plate; CCD, charge-coupled camera; and PCM, phase contrast microscopy.

makes the experimental setup a highly efficient workstation for waveguide writing.

After laser irradiation, the end facets of the created waveguides were grounded and polished and their transverse and longitudinal cross-sections were further analyzed using optical transmission (OTM) and cross-polarization microscopy (CPM) to characterize stress birefringence. The near-field modal investigation was performed using a typical end-face coupling arrangement with a 10× microscope objective. The near-field mode intensity profiles were recorded by imaging the output facets with a 20× microscope objective and a charge-coupled (CCD) camera. Waveguides were illuminated with polarized 800 nm CW light and an additional 980 nm fiber-pigtailed diode laser source.

## 3. Results and Discussion

In order to investigate the impact of the writing parameters on waveguide fabrication, we varied pulse duration, laser energy, and scan velocity across a wide parameter space of 120 fs to 1.5 ps, 0.7–4.2 μJ, and 5 μm/s to 640 μm/s, respectively. In comparison to the writing parameters of waveguides in fused silica glass or phosphate glass [18,19], the writing window of the SF10 glass is relatively broad. This section is organized as follows. Part A describes the impact of pulse duration on waveguide inscription in terms of refractive index change and the propagation loss of the waveguide. The pulse energy and scanning velocity effects on waveguide fabrication is investigated in part B. Part C presents the few-mode guiding phenomenon and discusses the formation condition and potential applications.

### A. Impact of Pulse Duration on Waveguide Fabrication

The modification tracks were inscribed at a depth of 100 μm inside the sample with 2.1 μJ pulse energy, 80 μm/s scan speed, and various pulse duration from 120 fs to 1.5 ps. Changing laser pulse duration had a significant effect on the waveguide morphology. With short pulse duration from 120 to 500 fs, no trace was observed in PCM microscope. With moderate pulse duration from 600 to 1200 fs, dark traces surrounded by weak negative refractive index claddings emerged, suggesting that high-quality waveguides could be obtained under this condition. Above 1200 fs, the propagation loss of the produced waveguides became large, associated with remarkably disordered modification tracks. No guiding was observed at pulse duration beyond the 1.5 ps. This behavior can be correlated with the interplay between carrier defocusing at short pulse duration, impeding energy deposition, and excitation efficiency at longer pulse duration.

Figure 2 depicts the overhead PCM images (top row) and the near-field mode images of the guided 980 nm light (bottom row) of the waveguides fabricated with the pulse duration from 600 to 1200 fs. As shown in Fig. 2, with the pulse duration of 600 and 700 fs, the waveguide is mainly made of a dark trace that represents a positive index change and indicates nearly symmetric Gaussian mode profiles with mode field diameters (MFDs) of 10.2–9.5 μm. As the pulse duration increases (above 800 fs), the negative refractive index (depressed) cladding surrounding the dark track appears, showing normally a uniform type of modification as noticeable in the PCM traces. Similar to [20–22], we attributed these morphology variations to a more effective material response to increasing pulse duration that can thus weaken nonlinear effects (e.g., self-focusing, defocusing, pulse breakup, filamentation, etc.) that reduce the efficiency at which energy can be deposited in the focal region and determine an increased energy deposition effectiveness, provided that excitation efficiency is sufficient. This pulse-dependent energy deposition rate also may be the reason for the non-observation of visible modification below 500 fs and above 1.5 ps. Two features are evident: the gray-level contrast in PCM increases with the pulse duration, indicating a variation of the index change and a marginal zone of negative index changes appears visible for picosecond pulse values. The MFDs decrease from 9.2 to 8.3 μm as the pulse duration



| 600fs | 700fs | 800fs | 900fs | 1ps | 1.1ps | 1.2ps |
|-------|-------|-------|-------|-----|-------|-------|

10μm

10μm

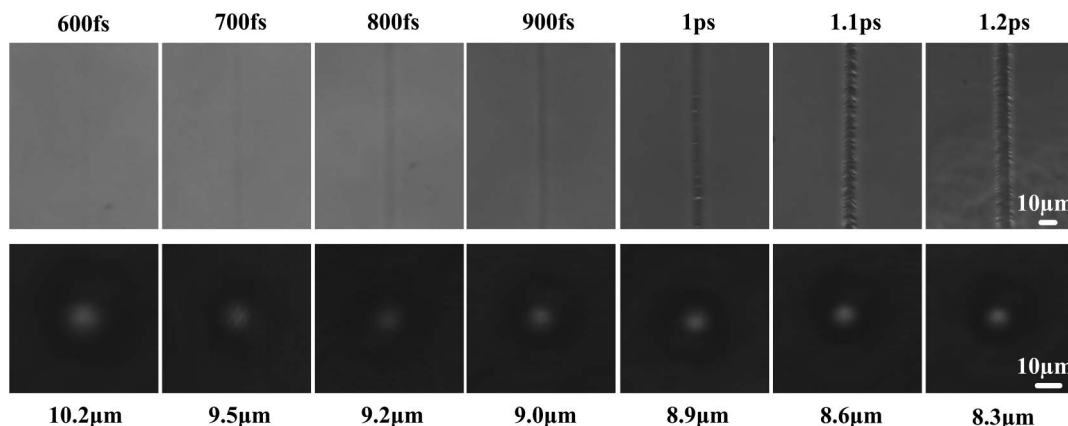| 10.2μm | 9.5μm | 9.2μm | 9.0μm | 8.9μm | 8.6μm | 8.3μm |
|--------|-------|-------|-------|-------|-------|-------|

Fig. 2. Waveguide laser fabrication results in SF10. Top row: side view PCM images of the laser generated traces. Bottom row: near-field mode images for injected 980 nm light of the waveguide written along the y axis for different writing pulse widths. Note the change in track morphology with the pulse duration.

increases, confirming the expected increase in the refractive index change with augmenting pulse duration. This change is reinforced from the combination of a rise in the refractive index of the core and the inward expansion of depressed cladding. The dark ring surrounding the guiding mode field shown in Fig. 2 arises from light refracted out of a lower refractive index cladding and scattered by the inhomogeneous structure.

The birefringence property of waveguide core and the regions in the vicinity of the modification tracks were checked with the cross-polarization microscope. The results show that these regions remain dark in the CPM images, indicating that the laser irradiation only produces a refractive index change without stress-induced birefringence being created in this waveguide fabrication procedure. This is different from the previously reported results [14,15], mainly because of the different glass composition and relatively low irradiation power density used in this work in the slit-shaping configuration. In order to investigate the impact of depressed cladding on the polarization guiding characteristics of the waveguide, both horizontally and vertically polarized light was injected into the waveguides. The results indicate that both modes can be guided with the same propagation loss, which confirms that the depressed cladding only introduces isotropic light scattering without polarization dependent loss.

To characterize index distribution, we reconstructed the refractive index profiles of the waveguides from their near-field modes according to the method described in [23]. In this method, the distribution of the refractive index change, $\Delta n(x,y)$, is given by

$$\Delta n(x,y) = \sqrt{n_s^2 - \frac{1}{k^2 E(x,y)} \nabla_t^2 E(x,y)} - n_s, \quad (1)$$

where $n_s$ is the refractive index of SF10 glasses, $k$ is wave number in a vacuum, and $E(x,y)$ is the normalized electric field intensity. The refractive index profile can be recovered by solving Eq. (1) using the finite differences method.

The reconstructed refractive index profile of the waveguide that was fabricated with 800 fs pulse duration is depicted in Fig. 3. As one can see, the center of the waveguide core corresponds to a maximum positive refractive index change of approximately $7.5 \times 10^{-4}$. The negative index change valley represents the depressed cladding, with a refractive index change of about $2.0 \times 10^{-4}$. The index contrast between the core and the cladding is therefore enhanced relative to the pristine material. As will be discussed later in part C, this negative index change in the cladding will contribute to the support of multiple propagation modes.

Figure 4 shows the measured maximum refractive index change in the waveguide core with different values of pulse duration. The change of refractive
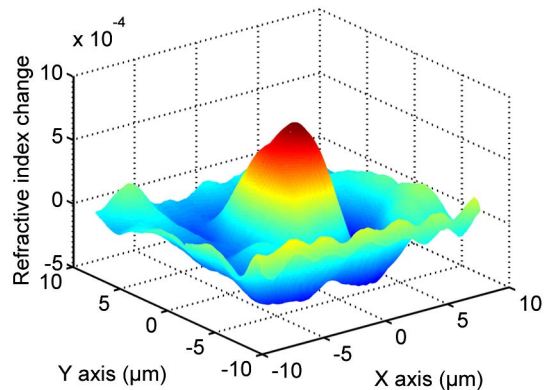


Fig. 3. Reconstructed refractive index distribution of the waveguide fabricated with 800 fs duration presented in Fig. 2. The red central peak represents the maximum refractive index change of up to $7.5 \times 10^{-4}$.

index increases with the increase of pulse duration. The core refractive index change of waveguides fabricated with pulse duration of <1000 fs is below $10^{-3}$, while for pulse duration of >1000 fs, the index change can be greater than $10^{-3}$ and becomes superlinear with respect to the increase of pulse duration. As indicated before, this result can be related to a behavior where early formed free carriers will defocus ultrashort laser pulses while longer pulses are able to confine better the energy and achieve higher excitation levels [20–22]. The value of refractive index change in this region is consistent with that reported in [14].

We use the cutback method [24] to measure the propagation loss of the waveguides. Waveguides with five different lengths were inscribed in the same sample. While each waveguide starts from the same facet of the sample that was carefully polished, the other end of each waveguide is inside the sample. The collimated 980 nm diode laser beam with an approximately Gaussian spatial distribution was coupled into the end of the selected waveguide inside the sample through an aspheric lens ($f = 15.29$ mm),
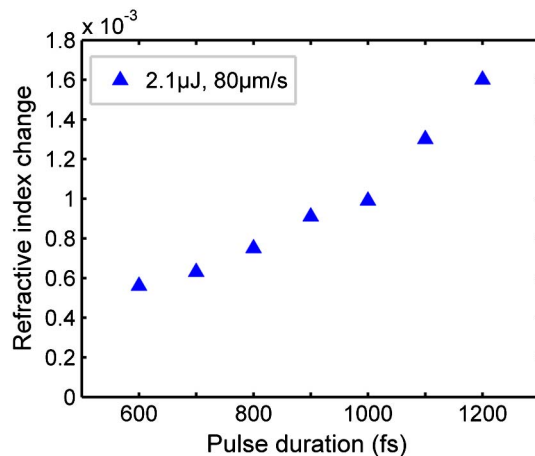


Fig. 4. Refractive index change as a function of the pulse duration for 2.1 μJ pulse energy and 80 μm/s scan speed.

which gives a diffraction limited pump spot size of about 7 μm ($1/e^2$ intensity diameter) at the focus, ensuring a moderate overlap efficiency between the pumping mode and the guiding mode. The output beam from the other end of the waveguide on the sample facet was collected by a 10× microscope objective.

The measured insertion loss of the waveguide shown in Fig. 2 with 800 fs laser pulse inscription is plotted against waveguide length in Fig. 5 and an equation of linear fit is shown for all lengths tested. The slope of this linear fit represents the propagation loss in decibel/centimeter and the *y* intercept gives the coupling loss due to mode field mismatch and the Fresnel reflection of both facets of the waveguide. As shown in Fig. 5, the low loss of 0.7 dB/cm implies a smooth track morphology of the waveguide. Two significant factors contributing to the 0.7 dB/cm loss are the scattering of the depressed cladding and mechanical instability of the motion stages. The coupling loss of 2.2 dB suggests a non-negligible mode field mismatch between the source and the waveguide.

Propagation losses corresponding to the waveguide writing conditions of Fig. 2 are plotted in Fig. 6 as a function of the pulse duration. The lowest propagation loss is ~0.7 dB/cm with pulse duration of 800 fs. Waveguides with lowest loss should correspond to the most homogeneous modification tracks and reasonable mode confinement, and, indeed, the top row of Fig. 2 shows waveguides with uniform tracks and smooth demarcations that were formed by pulse durations around 800 fs. Modest waveguide losses of <1 dB/cm are noted in a relatively wide processing window of 600–900 fs pulse duration, with a maximum loss of ~0.8 dB/cm in this range. Waveguiding was also observed for pulse duration beyond 1000 fs, but the propagation loss becomes large primarily due to the expanding of the depressed cladding (>2 μm). The disordered cladding may be responsible for scattering internally in the waveguides, contributing to the high propagation
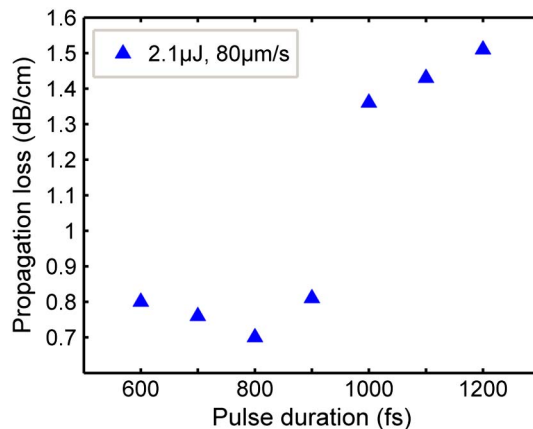


Fig. 6. Propagation loss as a function of the pulse duration for 2.1 μJ pulse energy and 80 μm/s scan speed.

losses (>1.5 dB/cm) observed here for long pulse durations (>1.2 ps) where nonuniform depressed claddings are evident.

Meanwhile, in view of the large dispersion of an SF10 sample, we checked the impact of the laser focusing depth into the sample on the waveguide writing. The laser was focused into a range of depths from 75 to 300 μm below the sample surface. It turned out that the change in the depth of laser foci and the amount of additional material crossed by the laser did not have an apparent influence on the waveguiding characteristic results. The results discussed above indicate that the window of pulse duration and local intensity on waveguide fabrication using SF10 is particularly wide and robust compared to other typical glass materials reported previously [18,19]. If the pulse duration is within this window centered on 0.8 ps, choosing an appropriate scan power and speed, low-loss waveguides can be obtained. To be noted here, due to the effect of spherical aberration originated from the high refractive index of SF10 glass ($n = 1.72$), the waveguide cross-sections became more asymmetric with deeper material penetration, an effect that can be corrected via slit dimensions.

## B. Pulse Energy and Scan Velocity Effects on Waveguide Fabrication

With an 800 fs pulse duration and a 80 μm/s scan speed, the impact of pulse energy on the waveguide property was examined across a wide range of values, from 0.7 to 4.2 μJ with 0.7 μJ increments. For pulse energies below 0.7 μJ, there was no clear evidence of index modification of the glass sample, suggesting that no waveguide could be obtained with these on-target pulse energy levels. For pulse energies of >4.2 μJ, inhomogeneous modification tracks appeared but with larger waveguide losses, indicating overexposure in these conditions. The structures written with pulse energy levels between these two extremes showed a uniform and continuous index modification in the glass, and low-loss waveguides could be created.
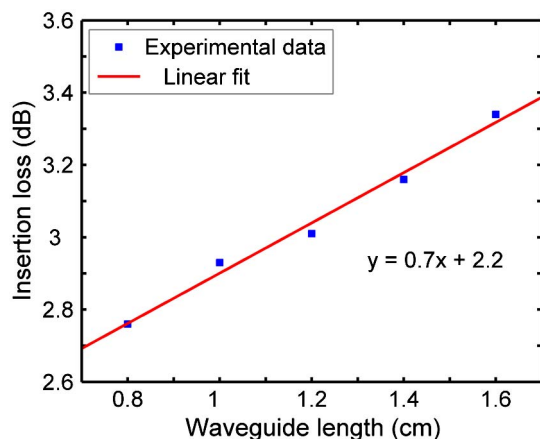


Fig. 5. Plot of insertion loss versus different waveguide lengths. The linear fit equation gives the propagation loss in decibel/centimeter (slope) and the coupling loss in decibel (y intercept).

Table [1] summarizes the MFDs ($1/e^2$ of peak intensity), the refractive index change, and the propagation loss. The MFDs range from 11.5 to 8.1 μm as the pulse energy enhances, presenting nearly symmetric Gaussian distribution profiles. At a pulse energy of 4.2 μJ, the refractive index change reaches up to $9.6 \times 10^{-4}$, with an 8.1 μm MFD and a relatively high propagation loss of 2 dB/cm. Similarly to the refractive index change, the propagation loss increases as the increase of the pulse energy. Note that for the pulse energy of above 2.8 μJ, the disordered cladding of negative refractive index change appears around the guiding region being responsible for propagation loss of >1 dB/cm, as shown in Table [1]. A minimum propagation loss of 0.65 dB/cm was found for the waveguide written with a 1.4 μJ pulse energy. The low loss of these waveguides suggests their potential use in integrated optical circuits, particularly for light transport and inherent dispersion compensation.

The impact of scan speed on waveguide fabrication was also investigated across a wide space from 5 to 640 μm/s, with the on-target energy being kept constant at 2.1 μJ and the pulse duration at 800 fs. The measured MFDs ($1/e^2$ of peak intensity), refractive index change, and the propagation loss in these conditions are summarized in Table [2]. Surprisingly, there is a very wide processing window of scan velocity from 5 to 640 μm/s. The MFDs increase gradually from 8.7 μm at 20 μm/s scan speed to 10.1 μm at 320 μm/s scan speed, indicating a slight dose-accumulation effect. The refractive index change ranges from $7.9 \times 10^{-4}$ to $6.5 \times 10^{-4}$, as shown in Table [2]. The propagation losses are below 0.9 dB/cm in this range with the lowest value of 0.7 dB/cm. Nevertheless, the best guiding mode properties of

**Table 1. Waveguide MFD, Refractive Index Change, and Loss at a 80 $\mu$m/s Scanning Velocity and a 800 fs Pulse Duration**

| Pulse Energy (μJ) | MFD (μm) | $\Delta n (\times 10^{-4})$ | Propagation Loss (dB/cm) |
|---|---|---|---|
| 0.7 | 11.5 | 5.1 | 0.81 |
| 1.4 | 10 | 6.5 | 0.65 |
| 2.1 | 9.0 | 7.5 | 0.7 |
| 2.8 | 8.9 | 9.1 | 0.86 |
| 3.5 | 8.5 | 11.6 | 1.39 |
| 4.2 | 8.1 | 13.5 | 2.0 |

**Table 2. Waveguide MFD, Refractive Index Change, and Loss at a 2.1 μJ Pulse Energy and a 800 fs Pulse Duration**

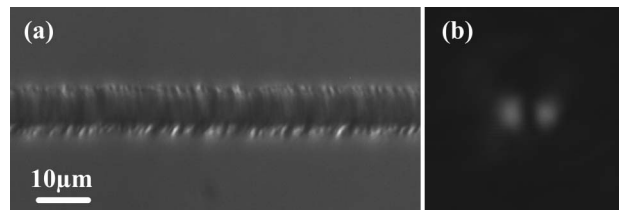| Scan Speed (μm/s) | MFD (μm) | $\Delta n (\times 10^{-4})$ | Propagation Loss (dB/cm) |
|---|---|---|---|
| 5 | 8.1 | 11.1 | 1.50 |
| 20 | 8.7 | 8.9 | 0.89 |
| 40 | 8.9 | 7.9 | 0.76 |
| 80 | 9.0 | 7.5 | 0.70 |
| 160 | 9.5 | 7.1 | 0.73 |
| 320 | 10.1 | 6.5 | 0.79 |
| 640 | 11.9 | 5.2 | 0.91 |



Fig. 7. LP$_{11}$ mode image of the waveguide for injected 800 nm radiation with a 10× objective, NA = 0.28.

the waveguide are obtained with a scanning speed between 40 and 160 μm/s.

In contrast to the high sensitivity to pulse duration and pulse energy, the results suggested that the waveguide properties are only weakly sensitive to the scan speed within 20 to 320 μm/s region for this waveguide writing scheme, and therefore the cumulative effects at low repetition rates are minimal.

### C. Few-Mode Guiding

In view of the before-mentioned facts in Fig. [4], the refractive index change can exceed $1.6 \times 10^{-3}$ with the writing condition of 2.1 μJ pulse energy, 80 μm/s scan speed, and 1200 fs pulse duration. Considering the negative refractive index change ($>0.2 \times 10^{-3}$) of the cladding, the index contrast between the core and the cladding should be greater. If we adopt writing parameters with higher pulse energy and lower scan speed, the index contrast could be large enough to support multiple-modes propagation. As was expected, with a 5 μm/s scan speed, 3.5 μJ pulse energy, and 1200 fs pulse duration, the first high-order modes (LP$_{11}$ mode) were observed for 800 nm signal wavelength. The PCM image and the near-field mode profile of the waveguide are depicted in Fig. [7]. The MFD is about 8 μm, and the cladding is obviously inhomogeneous. The propagation loss is up to 2.5 dB/cm due to scattering of the disordered depressing cladding.

Thus, relying on stable few-mode guiding and a simple single-scan writing technique, the fabricated structure is a promising candidate for future development of dispersion compensators, mode converters, and waveguide sensors [25] in the SF10 glass or other HMO glasses.

### 4. Conclusion

We have shown that optical waveguides with strong mode confinement, low losses, and symmetric refractive index profile can be fabricated in SF10 glass using a low-repetition-rate femtosecond laser writing. The impact of writing parameters on the waveguide formation in a transverse-writing slit-shaping scheme was systemically studied showing a large and robust processing window. Using index-profile reconstruction obtained by the measured near-field mode profile, a maximal refractive index modification of up to $1.6 \times 10^{-3}$ was obtained with 2.1 μJ pulse energy, 80 μm/s scan speed, and 800 fs pulse duration while still preserving low propagation losses. The propagation loss of the fabricated waveguides

were measured by the cutback method, with the lowest propagation loss being 0.7 dB/cm. Mostly SM propagation was obtained for NIR injection. In low-speed high-pulse energy and length conditions, large index contrast between the core and the cladding could be achieved, which supports few-mode propagation, i.e., $LP_{11}$ mode in the waveguide at 800 nm signal wavelength.

## References

1. K. M. Davis, K. Miura, N. Sugimoto, and K. Hirao, "Writing waveguides in glass with a femtosecond laser," Opt. Lett. **21**, 1729–1731 (1996).
2. R. R. Gattass and E. Mazur, "Femtosecond laser micromachining in transparent materials," Nat. Photonics **2**, 219–225 (2008).
3. R. R. Thomson and G. Cerullo, "Ultrafast laser inscription of photonic devices in bulk dielectrics," in *Ultrafast Nonlinear Optics* (Springer, 2013), Chap. 13, pp. 323–350.
4. H. Zhang, S. M. Eaton, and P. R. Herman, "Low-loss type II waveguide writing in fused silica with single picosecond laser pulses," Opt. Express **14**, 4826–4834 (2006).
5. M. Lancry, B. Poumellec, A. Chahid-Erraji, M. Beresna, and P. Kazansky, "Dependence of the femtosecond laser refractive index change thresholds on the chemical composition of doped-silica glasses," Opt. Mater. Express **1**, 711–723 (2011).
6. K. Mishchik, G. Cheng, G. Huo, I. M. Burakov, C. Mauclair, A. Mermillod-Blondin, A. Rosenfeld, Y. Ouerdane, A. Boukenter, O. Parriaux, and R. Stoian, "Nanosize structural modifications with polarization functions in ultrafast laser irradiated bulk fused silica," Opt. Express **18**, 24809–24824 (2010).
7. L. B. Fletcher, J. J. Witcher, N. Troy, S. T. Reis, R. K. Brow, and D. M. Krol, "Direct femtosecond laser waveguide writing inside zinc phosphate glass," Opt. Express **19**, 7929–7936 (2011).
8. R. R. Thomson, S. Campbell, I. J. Blewett, A. K. Kar, and D. T. Reid, "Optical waveguide fabrication in z-cut lithium niobate ($LiNbO_3$) using femtosecond pulses in the low repetition rate regime," Appl. Phys. Lett. **88**, 111109 (2006).
9. Y. Tan, Y. C. Jia, F. Chen, J. R. Vázquez de Aldana, and D. Jaque, "Simultaneous dual-wavelength lasers at 1064 and 1342 nm in femtosecond-laser-written $Nd:YVO_4$ channel waveguides," J. Opt. Soc. Am. B **28**, 1607–1610 (2011).
10. A. Rodenas and A. K. Kar, "High-contrast step-index waveguides in borate nonlinear laser crystals by 3D laser writing," Opt. Express **19**, 17820–17833 (2011).
11. D. G. Lancaster, S. Gross, H. Ebendorff-Heidepriem, K. Kuan, T. M. Monro, M. Ams, A. Fuerbach, and M. J. Withford, "Fifty percent internal slope efficiency femtosecond direct-written $Tm^{3+}$:ZBLAN waveguide laser," Opt. Lett. **36**, 1587–1589 (2011).
12. T. Calmano, A. G. Paschke, J. Siebenmorgen, S. T. Fredrich-Thornton, H. Yagi, K. Petermann, and G. Huber, "Characterization of an Yb:YAG ceramic waveguide laser, fabricated by the direct femtosecond-laser writing technique," Appl. Phys. B **103**, 1–4 (2011).
13. L. Kallepalli, V. Soma, and N. Desai, "Femtosecond-laser direct writing in polymers and potential applications in microfluidics and memory devices," Opt. Eng. **51**, 073402 (2012).
14. J. Siegel, J. M. Fernandez-Navarro, A. García-Navarro, V. Diez-Blanco, O. Sanz, J. Solis, F. Vega, and J. Armengol, "Waveguide structures in heavy metal oxide glass written with femtosecond laser pulses above the critical self-focusing threshold," Appl. Phys. Lett. **86**, 121109 (2005).
15. V. Diez-Blanco, J. Siegel, and J. Solis, "Waveguide structures written in SF57 glass with fs-laser pulses above the critical self-focusing threshold," Appl. Surf. Sci. **252**, 4523–4526 (2006).
16. R. R. Thomson, N. D. Psaila, S. J. Beecher, and A. K. Kar, "Ultrafast laser inscription of a high-gain Er-doped bismuthate glass waveguide amplifier," Opt. Express **18**, 13212–13219 (2010).
17. M. Ams, G. Marshall, D. Spence, and M. Withford, "Slit beam shaping method for femtosecond laser direct-write fabrication of symmetric waveguides in bulk glasses," Opt. Express **13**, 5676–5681 (2005).
18. G. Cheng, K. Mishchik, C. Mauclair, E. Audouard, and R. Stoian, "Ultrafast laser photoinscription of polarization sensitive devices in bulk silica glass," Opt. Express **17**, 9515–9525 (2009).
19. J. W. Chan, T. R. Huser, S. H. Risbud, J. S. Hayden, and D. M. Krol, "Waveguide fabrication in phosphate glasses using femtosecond laser pulses," Appl. Phys. Lett. **82**, 2371–2373 (2003).
20. A. Mermillod-Blondin, C. Mauclair, A. Rosenfeld, J. Bonse, I. V. Hertel, E. Audouard, and R. Stoian, "Size correction in ultrafast laser processing of fused silica by temporal pulse shaping," Appl. Phys. Lett. **93**, 021921 (2008).
21. A. H. Nejadmalayeri and P. R. Herman, "Ultrafast laser waveguide writing: lithium niobate and the role of circular polarization and picosecond pulse width," Opt. Lett. **31**, 2987–2989 (2006).
22. J. R. Macdonald, R. R. Thomson, S. J. Beecher, N. D. Psaila, H. T. Bookey, and A. K. Kar, "Ultrafast laser inscription of near-infrared waveguides in polycrystalline ZnSe," Opt. Lett. **35**, 4036–4038 (2010).
23. F. Caccavale, F. Segato, I. Mansour, and M. Gianesin, "A finite differences method for the reconstruction of refractive index profiles from near-field measurements," J. Lightwave Technol. **16**, 1348–1353 (1998).
24. L. Shah, A. Arai, S. Eaton, and P. Herman, "Waveguide writing in fused silica with a femtosecond fiber laser at 522 nm and 1 MHz repetition rate," Opt. Express **13**, 1999–2006 (2005).
25. M. Spajer and B. Charquille, "Application of intermodal interference to fiber sensors," Opt. Commun. **60**, 261–264 (1986).